THE AMERICAN MINERALOGIST
JOURNAL OF THE MINERALOGICAL SOCIETY OF AMERICA

Vol. 26 AUGUST, 1941 No. 8

THE ATOMIC ARRANGEMENT OF SYLVANITE

GEORGE TUNELL,
Geophysical Laboratory, Carnegie Institution of Washington.

ABSTRACT

The crystal structure of sylvanite has been analyzed by means of Weissenberg photographs and powder diffraction photographs. The dimensions of the unit cell, all determined by purely röntgenographic measurements, are $a_0=8.94$ Å, $b_0=4.48$ Å, $c_0=14.59$ Å, all ± 0.02 Å, and $\beta=145°26' \pm 20'$. The density measured by Palache is 8.16; the corresponding x-ray density is 8.17. The unit cell contains $2AuAgTe_4$, and a small part of the silver atoms required by this ideal formula is replaced by gold atoms. The space-group is C_{2h}^4-P2/c. The seven parameters defining the atomic positions were determined by calculation of the intensities of the diffraction lines of the powder spectrum (which had been rigorously indexed from the single crystal data), and of the diffraction spots of Weissenberg equator photographs of crystals rotating about the a-axis and [201] zone-axis; the positions of the atoms were confirmed by a Fourier projection of the structure on the plane 010 made from a Weissenberg equator photograph taken with the crystal rotating about the b-axis. The gold atoms are situated in (a) 000; $00\frac{1}{2}$, the silver atoms in (e) $0y\frac{1}{4}$; $0\bar{y}\frac{3}{4}$, with $y=0.433$, and the two sets of tellurium atoms in (g) xyz; $\bar{x}\bar{y}\bar{z}$; $\bar{x}$, y, $\frac{1}{2}-z$; x, $\bar{y}$, $\frac{1}{2}+z$, with $x_1=0.298$, $y_1=0.031$, $z_1=0.999$, and $x_2=0.277$, $y_2=0.425$, $z_2=0.235$. Each gold atom and each silver atom is surrounded octahedrally by six tellurium atoms, and each tellurium atom is surrounded octahedrally by three tellurium atoms, two gold atoms, and one silver atom, or by three tellurium atoms, two silver atoms, and one gold atom.

INTRODUCTION

The atomic arrangement of sylvanite has been determined in the present investigation by röntgenographic analysis of faceted crystals from Cripple Creek, Colorado,[1] from Săcărâmbu (Nagy-Ág), Transilvania (Siebenbürgen),[2] and from the Buena Mine, Jamestown District, Colorado.[3] The crystals had a metallic luster and steel grey color; their identity was confirmed by measurement on the two-circle reflection goniometer. New crystallographic axes were chosen for use in the structural investigation to conform with the arrangement of the symmetry elements assumed in the "Internationale Tabellen zur Bestimmung von Kristall-

[1] Kindly supplied by Professor Charles Palache of Harvard University.

[2] Kindly furnished by Dr. W. F. Foshag of the United States National Museum.

[3] Obtained through the kindness of Dr. E. N. Goddard of the United States Geological Survey.

strukturen."[4] The axes of Schrauf[5] are not those of a possible unit cell in the structure and for this reason were not retained for purposes of structural analysis. Schrauf's axes are related to the structural axes by the following transformation:

Schrauf to Tunell $\bar{\frac{1}{2}}0\frac{1}{2}/0\bar{\frac{1}{2}}0/100$.[6]

Rotation and Weissenberg equator and layer-line photographs were made with crystals rotating about the *a*-axis, *b*-axis, and [201] zone-axis.[7] Copper K-radiation was used except that a rotation photograph about the *a*-axis was also made with chromium K-radiation and an equator Weissenberg photograph about the [201] zone-axis with molybdenum K-radiation. Powder photographs were made with filtered and unfiltered copper K-radiation. The crystal of which the first Weissenberg photographs were made came from Cripple Creek, Colorado; it was rotated about the *a*-axis, and equator and layer-line Weissenberg photographs were made. The preliminary measurement on the two-circle reflection goniometer showed that it was elongated parallel to the *a*-axis[8] and twinned according to the common law for sylvanite, twinning plane {001},[9] and the graphical construction of the layers of the reciprocal lattice from the Weissenberg photographs by the method of Schneider[10] confirmed the twin-law. A powder photograph with unfiltered copper K-radiation was made of this crystal. Single crystals were obtained from a specimen from Săcărâmbu (Nagy-Ág);[11] one was elongated parallel to the *a*-axis and was bounded by several good faces in the zone parallel to this axis and one cleavage parallel to {010}; this cleavage was the surface along which the crystal had been broken off. The cross section of the crystal perpendicular to the *a*-axis had approximately equal diameters in all directions (about 0.1 mm.). Rotation and equator and layer-line Weissenberg photographs were made with this crystal rotating about the *a*-axis. Another single crystal from the same specimen was elongated parallel to the [201] zone-axis[12] and was approximately equi-dimensional in cross section (about 0.05 mm. in diameter); rotation and equator and layer-line Weissenberg photographs were made with this crystal rotating about the [201] zone-axis. A cleavage fragment from the specimen from

[4] Internationale Tabellen zur Bestimmung von Kristallstrukturen, Gebrüder Borntraeger, *Berlin*, p. 101 **(1935).**

[5] *Zeits. Krist.*, **2,** 209–252 (1878).

[6] For the reason for the fractional form see M. A. Peacock: *Am. Mineral.*, **23,** 38 (1938).

[7] All letters and symbols in this paper refer to the structural lattice and the unit cell described in the following section except where a statement is made to the contrary.

[8] This is the [$\bar{1}$01] zone-axis of Schrauf.

[9] This plane has the symbol {101} when referred to the axes of Schrauf.

[10] *Zeits. Krist.*, **69,** 41–48 (1928).

[11] U. S. National Museum, No. R916.

[12] This is the *c*-axis of Schrauf.

Săcărâmbu (Nagy-Ág) was rotated about the *b*-axis, and a rotation and an equator Weissenberg photograph were obtained; the equator Weissenberg photograph showed that this fragment was twinned with the twinning plane {001}. Powder photographs of a sample from this specimen were made with filtered copper K-radiation. Lastly, a well-developed single crystal from the Buena Mine, Jamestown District, Colorado, was measured completely on the two-circle reflection goniometer; its cross section perpendicular to the *b*-axis is roughly triangular, and the average diameter of this cross section is approximately 0.5 mm. Rotation and Weissenberg equator and layer-line photographs were made with this crystal rotating about the *b*-axis, and a rotation and an equator Weissenberg photograph with the crystal rotating about the [201] zone-axis. A search was made for a smaller crystal that could be rotated about the *b*-axis, but none suitable for this purpose could be found.

Determination of the Unit Cell and Space-Group

The dimensions of the structural unit cell, all determined by purely röntgenographic measurements, are $a_0 = 8.94$ Å, $b_0 = 4.48$ Å, $c_0 = 14.59$ Å, all ± 0.02 Å; $\beta = 145°26' \pm 20'$.[13] The volume of the unit cell is accordingly 331.6 Å^3. The chemical analysis of crystallographically studied material from the Cripple Creek District, Colorado, made by Palache[14] corresponds to the composition (Au, Ag)Te_2 with an atomic ratio of gold to silver equal to 1.15. The density determined by Palache[15] on three isolated crystals by means of the hydrostatic balance is 8.16. The density computed from the *x*-ray measurements with use of the ideal formula $AuAgTe_4$ is 8.11; if the ratio of gold to silver is taken as 1.15 (corresponding to the analysis of Palache) instead of 1.00 (corresponding to the ideal formula), and if, as appears very probable, the slight excess of gold is the result of replacement of silver atoms by gold atoms in the structure, the *x*-ray density is 8.17. The agreement of the measured density with this calculated density leaves no doubt that the content of the unit cell is $2AuAgTe_4$, and confirms the assumption that the slight excess of gold over that required by the ideal formula and the slight deficiency of silver is the result of replacement of part of the silver atoms by gold atoms. Diffraction effects were obtained on the Weissenberg photographs from the following planes: *u*00, *g*00, 0*u*0, 0*g*0, 00*g*, 0*uu*, 0*ug*, 0*gu*, 0*gg*, *u*0*g*, *g*0*g*, *ug*0, *gu*0, *gg*0, *uu*0,[16] *uuu*, *uug*, *ugu*, *ugg*, *guu*, *gug*, *ggu*, *ggg*, where *u* de-

[13] Tunell, G. and Ksanda, C. J.: *Am. Mineral.*, **22,** 728 (1937).

[14] *Am. Jour. Sci.*, (4), **10,** 422 (1900).

[15] *Am. Jour. Sci.*, (4), **10,** 419 (1900).

[16] It was reported previously (*Am. Mineral.*, **22,** 728 (1937)) that no diffraction effects were obtained from planes having indices *uu*0. The statement was based on examination of a Weissenberg photograph of the first layer-line (crystal rotating about the *a*-axis). Since

notes any odd number and g denotes any even number. No diffraction effects were obtained from the following: $00u$, $u0u$, $g0u$, although representatives of each were in a position to diffract. Thus sylvanite belongs either to the space-group C_s^2-Pc or to the space-group C_{2h}^4-P2/c, both of which are characterized by the absence of diffraction effects from $00u$, $u0u$, and $g0u$, due to the presence of a glide plane parallel to 010 with a glide component of $c/2$. Faceted crystals of sylvanite have been studied with the reflection goniometer by several investigators. Projections of such crystals drawn by Koksharov, Schrauf, Vrba, and Palache and reproduced by V. Goldschmidt in his "Atlas der Krystallformen"[17] show the habit of sylvanite to be holohedral. Morphological study of crystals used in the present röntgenographic investigation also indicates the presence of a two-fold axis and consequently points to holohedral symmetry. Hence the space-group of sylvanite is C_{2h}^4-P2/c.

Determination of the Atomic Arrangement

There are two gold, two silver, and eight tellurium atoms to be located in the unit cell. The space-group C_{2h}^4-P2/c furnishes the following sets of equivalent positions:

(a) 000; $00\frac{1}{2}$; (b) $\frac{1}{2}\frac{1}{2}0$; $\frac{1}{2}\frac{1}{2}\frac{1}{2}$; (c) $0\frac{1}{2}0$; $0\frac{1}{2}\frac{1}{2}$;
(d) $\frac{1}{2}00$; $\frac{1}{2}0\frac{1}{2}$; (e) $0y\frac{1}{4}$; $0\bar{y}\frac{3}{4}$; (f) $\frac{1}{2}y\frac{1}{4}$; $\frac{1}{2}\bar{y}\frac{3}{4}$;
(g) xyz; $\bar{x}\bar{y}\bar{z}$; $\bar{x}$, y, $\frac{1}{2}-z$; x, $\bar{y}$, $\frac{1}{2}+z$;

of which (a), (b), (c), and (d) have the symmetry C_i, (e) and (f) the symmetry C_2, and (g) the symmetry C_1. Several different arrangements of the atoms in these positions are possible with reasonable interatomic distances. Only one of these arrangements could be found, however, that yields calculated intensities in agreement with those observed. This arrangement is the following: gold atoms in (a) 000, $00\frac{1}{2}$; silver atoms in (e) $0y\frac{1}{4}$, $0\bar{y}\frac{3}{4}$; with $y=0.433$; and two sets of tellurium atoms in (g) xyz; $\bar{x}\bar{y}\bar{z}$; $\bar{x}$, y, $\frac{1}{2}-z$; x, $\bar{y}$, $\frac{1}{2}+z$, with $x_1=0.298$, $y_1=0.031$, $z_1=0.999$, and $x_2=0.277$, $y_2=0.425$, $z_2=0.235$. Orthographic projections of this structure are given in Fig. 1, and a model of the structure is shown in Fig. 2.[18] The intensities calculated[19] from this structure are compared with those observed in Tables I, II, III, and IV. Table I contains the observed and calculated intensities of diffraction lines on a powder photograph taken

then a Weissenberg photograph of the third layer-line (crystal rotating about the a-axis) has been made and diffraction effects have been found from planes having indices $uu0$. This does not alter any of the conclusions previously drawn.

[17] Carl Winters Universitätsbuchhandlung, *Heidelberg* (**1922**), Band VIII, Tafeln 65–68.

[18] The author is indebted to Mr. H. A. Schmidt, Jr. for the skillful construction of this model.

[19] The author acknowledges with appreciation the painstaking assistance Mrs. R. P. Tunell has rendered in performing the lengthy calculations.

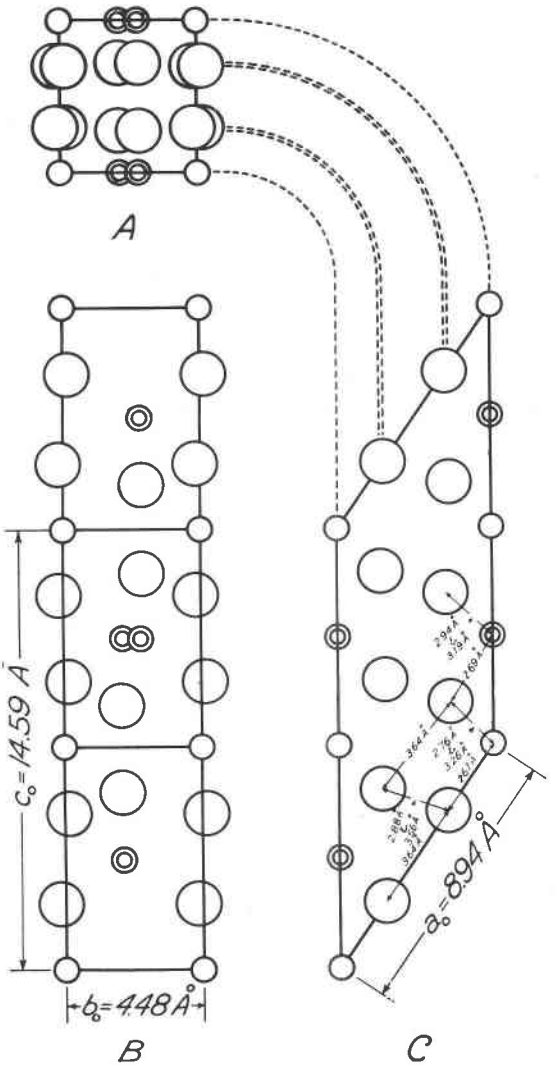

FIG. 1. Orthographic projections of the unit cell of sylvanite. A. Top view. B. Front view. C. Side view. Small single circles—gold atoms. Small double circles—silver atoms. Large circles—tellurium atoms.

with copper K-radiation filtered through nickel foil. The indexing of the powder photograph was carried out rigorously by use of the unit cell dimensions obtained from the single crystal Weissenberg photographs.

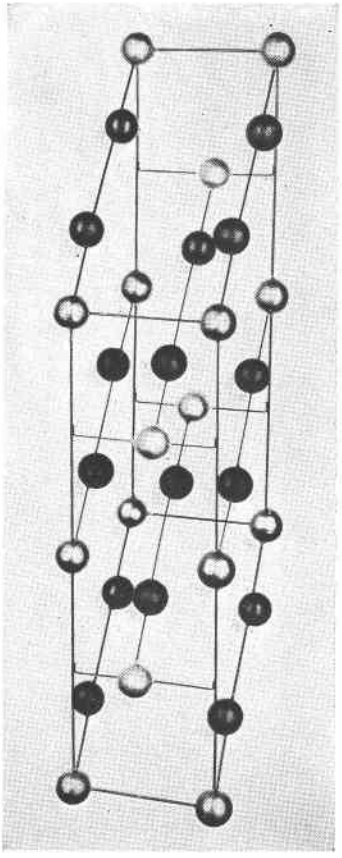

FIG. 2. Model showing the arrangement of the atoms in sylvanite. The parallelepiped represented by the outside wires is the unit cell. The *a*-axis slopes from back to front; the *b*-axis extends from left to right; and the *c*-axis is vertical. The dark grey spheres represent gold atoms; the light grey spheres represent silver atoms; the black spheres represent tellurium atoms.

Table I lists in decreasing order the calculated and observed spacings and intensities of all planes the spacings of which are greater than 1.378 Å, together with the observed spacings and intensities of the remaining lines of the powder photograph. The intensities I_P of the lines on the powder diffraction film taken with filtered radiation were calculated from the formula

$$I_P = \frac{1 + \cos^2 2\theta}{\sin 2\theta} j \mid F \mid^2,$$

TABLE I

Relative intensities* of the x-ray diffraction lines of sylvanite from a powder photograph taken with filtered copper K-radiation.

Indices *hkl*	Spacing calculated	Relative intensity calculated	Spacing measured	Relative intensity observed
$10\bar{1}$	8.382	0.0		
001	8.278	0.0		
$10\bar{2}$	7.295	0.2		
100	5.072	0.7	5.102	1
010	4.480	0.2		
$20\bar{3}$	4.408	0.0		
$10\bar{3}$	4.363	0.0		
$20\bar{2}$	4.190	0.1		
002	4.139	0.1		
$11\bar{1}$	3.951	0.0		
011	3.940	0.7	3.970	$\frac{1}{2}$
$11\bar{2}$	3.818	0.6	3.851	$\frac{1}{2}$
$20\bar{4}$	3.647	0.1		
110	3.358	0.1		
$20\bar{1}$	3.304	0.0		
101	3.285	0.0		
$21\bar{3}$	3.142	0.1		
$11\bar{3}$	3.126	0.0		
$21\bar{2}$	3.060	0.1		
012	3.040	9.9	3.045	10
$30\bar{4}$	2.980	3.9	2.976	6
$10\bar{4}$	2.943	0.1		
$21\bar{4}$	2.828	0.0		
$30\bar{5}$	2.814	0.0		
$30\bar{3}$	2.794	0.0		
$20\bar{5}$	2.794	0.0		
003	2.759	0.0		
$21\bar{1}$	2.659	0.0		
111	2.649	0.1		
200	2.536	0.1		
$31\bar{4}$	2.481	0.1		
$11\bar{4}$	2.460	0.2		
$30\bar{6}$	2.432	0.0		
$30\bar{2}$	2.405	0.0		
102	2.386	0.0		
$31\bar{5}$	2.383	0.3		
$21\bar{5}$	2.371	0.0	2.367	$\frac{1}{2}$
$31\bar{3}$	2.370	0.1		
013	2.349	0.3		
020	2.240	2.0	2.244	3
$40\bar{5}$	2.224	0.0		
210	2.207	0.1		

TABLE I—*Continued*

Indices *hkl*	Spacing calculated	Relative intensity calculated	Spacing measured	Relative intensity observed
$40\bar{6}$	2.204	0.0		
$10\bar{5}$	2.195	0.0		
$20\bar{6}$	2.181	0.0		
$12\bar{1}$	2.164	0.1		
021	2.162	0.7		
$12\bar{2}$	2.141	0.1	2.149	5
$31\bar{6}$	2.137	4.1		
$31\bar{2}$	2.122	3.5	2.118	5
112	2.106	0.5		
$40\bar{4}$	2.095	1.2		
004	2.070	2.6	2.076	3
120	2.049	0.3		
$40\bar{7}$	2.047	0.0		
$30\bar{7}$	2.036	0.0		
$30\bar{1}$	2.013	0.0		
201	2.006	0.0		
$22\bar{3}$	1.997	0.0		
$12\bar{3}$	1.993	0.1		
$41\bar{5}$	1.992	0.0		
$41\bar{6}$	1.978	1.7	1.983	4
$22\bar{2}$	1.976	0.0		
$11\bar{5}$	1.971	0.0		
022	1.970	0.3		
$21\bar{6}$	1.961	0.0		
$22\bar{4}$	1.909	0.0		
$41\bar{4}$	1.898	0.0		
$40\bar{3}$	1.881	0.0		
014	1.879	0.1		
103	1.864	0.0		
$41\bar{7}$	1.862	0.1		
$22\bar{1}$	1.854	0.2		
$31\bar{7}$	1.854	0.1		
121	1.851	0.0	1.844	1
$31\bar{1}$	1.836	0.1		
211	1.831	0.0		
$40\bar{8}$	1.824	0.6		
$32\bar{4}$	1.791	1.9	1.796	2
$50\bar{7}$	1.785	0.0		
$12\bar{4}$	1.782	0.1		
$50\bar{6}$	1.767	0.0		
$20\bar{7}$	1.764	0.0		
$32\bar{5}$	1.752	0.2		
$22\bar{5}$	1.748	0.1		
$32\bar{3}$	1.748	0.5		
$10\bar{6}$	1.744	0.1		

TABLE I—*Continued*

Indices *hkl*	Spacing calculated	Relative intensity calculated	Spacing measured	Relative intensity observed
023	1.739	0.4		
41$\bar{3}$	1.735	0.1		
50$\bar{8}$	1.723	0.1	1.727	1 (broad)
113	1.721	0.0		
30$\bar{8}$	1.709	1.5	1.687	
300	1.691	1.0		½
41$\bar{8}$	1.689	0.1		
220	1.679	0.0		
50$\bar{5}$	1.676	0.0		
005	1.656	0.0		
40$\bar{2}$	1.652	0.0		
51$\bar{7}$	1.648	0.0		
32$\bar{6}$	1.648	0.1		
51$\bar{6}$	1.644	0.1		
202	1.642	0.0		
21$\bar{7}$	1.641	0.0		
32$\bar{2}$	1.640	0.2		
122	1.633	0.0		
11$\bar{6}$	1.625	0.0		
51$\bar{8}$	1.608	0.0		
50$\bar{9}$	1.604	0.0		
40$\bar{9}$	1.597	0.0		
31$\bar{8}$	1.597	0.0		
310	1.582	0.1		
42$\bar{5}$	1.578	0.3		
42$\bar{6}$	1.571	0.1		
51$\bar{5}$	1.570	0.0		
12$\bar{5}$	1.568	0.0		
22$\bar{6}$	1.563	0.0		
015	1.553	0.1		
41$\bar{2}$	1.550	1.2		
212	1.542	0.1		
50$\bar{4}$	1.542	0.1		
42$\bar{4}$	1.530	0.8	1.524	
104	1.526	0.2		3
024	1.520	1.7		
42$\bar{7}$	1.511	0.0		
51$\bar{9}$	1.510	0.0		
32$\bar{7}$	1.507	0.4		
41$\bar{9}$	1.505	0.0		
32$\bar{1}$	1.497	0.1		
221	1.494	0.0		
030	1.493	0.2	1.494	½
60$\bar{8}$	1.490	0.3		
20$\bar{8}$	1.472	0.0		

TABLE I—*Continued*

Indices *hkl*	Spacing calculated	Relative intensity calculated	Spacing measured	Relative intensity observed
$13\bar{1}$	1.470	0.0		
031	1.470	0.5		
$60\bar{9}$	1.469	0.0		
$60\bar{7}$	1.464	0.0		
$13\bar{2}$	1.463	0.1		
$5.0.\bar{10}$	1.459	0.0		
$51\bar{4}$	1.458	0.0		
$30\bar{9}$	1.454	0.0		
114	1.445	0.0		
$10\bar{7}$	1.444	0.0		
$40\bar{1}$	1.444	0.0		
$42\bar{3}$	1.441	0.0		
301	1.440	0.0		
123	1.433	0.1		
130	1.432	0.0		
$23\bar{3}$	1.414	0.1		
$42\bar{8}$	1.414	0.5		
$61\bar{8}$	1.414	0.0		
$13\bar{3}$	1.413	0.1	1.413	1 (broad)
$6.0.\bar{10}$	1.407	0.0		
$23\bar{2}$	1.407	0.0		
032	1.405	0.6		
$21\bar{8}$	1.398	0.0		
$4.0.\bar{10}$	1.397	0.1		
$60\bar{6}$	1.397	0.0		
$61\bar{9}$	1.396	0.0		
$52\bar{7}$	1.396	0.0		
$50\bar{3}$	1.394	0.0		
$61\bar{7}$	1.391	0.0		
$52\bar{6}$	1.387	0.0		
$5.1.\bar{10}$	1.387	0.1		
$22\bar{7}$	1.386	0.0		
203	1.384	0.0		
$31\bar{9}$	1.383	0.1		
$23\bar{4}$	1.382	0.0		
006	1.380	0.0		
			1.364	$\frac{1}{2}$
			1.345	2
			1.324	2
			1.269	1
			1.245	1
			1.222	2
			1.197	1
			1.088	2

TABLE I—*Continued*

Indices *hkl*	Spacing calculated	Relative intensity calculated	Spacing measured	Relative intensity observed
			1.050	½
			1.020	1
			0.977	½ (broad)
			0.897	1
			0.873	1
			0.822	1

* The intensities were estimated visually on a scale of ten, where ten represents the intensity of the strongest line.

TABLE II

Relative intensities of *x*-ray diffraction spots from a Weissenberg equator photograph of sylvanite taken with the crystal rotating around the *a*-axis.

Indices *hkl*	Spacing calculated	Relative intensity		CuK-radiation †
		observed*	calculated	
001	8.278	0	0.0	$\alpha_1+\alpha_2$
002	4.139	0	0.2	$\alpha_1+\alpha_2$
003	2.759	0	0.0	$\alpha_1+\alpha_2$
004	2.070	s	5.3	$\alpha_1+\alpha_2$
005	1.656	0	0.0	$\alpha_1+\alpha_2$
006	1.380	0	0.0	$\alpha_1+\alpha_2$
007	1.183	0	0.0	$\alpha_1+\alpha_2$
008	1.035	m	0.7	α_1
009	0.920	0	0.0	α_1
0.0.10	0.828	w	0.1	α_1
010	4.480	w	0.4	$\alpha_1+\alpha_2$
020	2.240	s	4.1	$\alpha_1+\alpha_2$
030	1.493	m	0.4	$\alpha_1+\alpha_2$
040	1.120	w	0.2	$\alpha_1+\alpha_2$
050	0.896	m	0.5	α_1
011	3.940	w	0.7	$\alpha_1+\alpha_2$
012	3.040	s	10.0	$\alpha_1+\alpha_2$
013	2.349	w	0.3	$\alpha_1+\alpha_2$
014	1.879	w	0.1	$\alpha_1+\alpha_2$
015	1.553	w	0.1	$\alpha_1+\alpha_2$
016	1.318	m	1.6	$\alpha_1+\alpha_2$
017	1.143	0	0.0	$\alpha_1+\alpha_2$
018	1.008	w	0.1	$\alpha_1+\alpha_2$
019	0.901	0	0.0	α_1
0.1.10	0.814	s	1.2	α_1

TABLE II—*Continued*

Indices *hkl*	Spacing calculated	Relative intensity		CuK-radiation†
		observed*	calculated	
021	2.162	w	0.8	$\alpha_1+\alpha_2$
022	1.970	w	0.3	$\alpha_1+\alpha_2$
023	1.739	w	0.4	$\alpha_1+\alpha_2$
024	1.520	m	1.7	$\alpha_1+\alpha_2$
025	1.331	w	0.2	$\alpha_1+\alpha_2$
026	1.175	w	0.1	$\alpha_1+\alpha_2$
027	1.046	w	0.1	$\alpha_1+\alpha_2$
028	0.939	m	0.5	α_1
029	0.851	0	0.1	α_1
031	1.470	w	0.5	$\alpha_1+\alpha_2$
032	1.405	m	0.6	$\alpha_1+\alpha_2$
033	1.313	w	0.3	$\alpha_1+\alpha_2$
034	1.211	w	0.3	$\alpha_1+\alpha_2$
035	1.109	0	0.2	$\alpha_1+\alpha_2$
036	1.013	w	0.4	$\alpha_1+\alpha_2$
037	0.927	0	0.1	α_1
038	0.850	m	0.2	α_1
039	0.783	w	0.4	α_1
041	1.110	0	0.3	$\alpha_1+\alpha_2$
042	1.081	m	0.3	α_1
043	1.038	0	0.2	α_1
044	0.985	w	0.1	α_1
045	0.928	0	0.2	α_1
046	0.870	m	0.4	α_1
047	0.813	0	0.3	α_1
051	0.891	0	0.1	α_1
052	0.876	0	0.0	α_1
053	0.852	0	0.1	α_1
054	0.822	m	0.8	α_1
055	0.788	0	0.3	α_1

* Denotation of symbols: s, strong; m, medium; w, weak.

† The symbol $\alpha_1+\alpha_2$ denotes an unresolved spot resulting from α_1 and α_2 rays together; the symbol α_1 denotes a spot resulting from α_1 rays alone.

TABLE III

Relative intensities of x-ray diffraction spots from a Weissenberg equator photograph of sylvanite taken with the crystal rotating around the b-axis.

Indices *hkl*	Spacing calculated	Relative intensity		CuK-radiation
		observed	calculated	
100	5.072	w	1.8	$\alpha_1+\alpha_2$
200	2.536	w	0.2	$\alpha_1+\alpha_2$
300	1.691	s	2.6	$\alpha_1+\alpha_2$
400	1.268	m	1.2	$\alpha_1+\alpha_2$
500	1.014	w	0.0	α_1
600	0.845	w	0.1	α_1
$10\bar{2}$	7.295	w	0.5	$\alpha_1+\alpha_2$
$20\bar{4}$	3.647	w	0.2	$\alpha_1+\alpha_2$
$30\bar{6}$	2.432	0	0.0	$\alpha_1+\alpha_2$
$40\bar{8}$	1.824	s	1.6	$\alpha_1+\alpha_2$
$5.0.\bar{1}0$	1.459	w	0.0	$\alpha_1+\alpha_2$
$6.0.\bar{1}2$	1.216	m	0.7	$\alpha_1+\alpha_2$
$7.0.\bar{1}4$	1.042	w	0.0	α_1
$8.0.\bar{1}6$	0.912	w	0.0	α_1
$9.0.\bar{1}8$	0.811	w	0.0	α_1
002	4.139	w	0.2	$\alpha_1+\alpha_2$
$10\bar{4}$	2.943	w	0.3	$\alpha_1+\alpha_2$
$20\bar{6}$	2.181	0	0.0	$\alpha_1+\alpha_2$
$30\bar{8}$	1.709	s	3.8	$\alpha_1+\alpha_2$
$4.0.\bar{1}0$	1.397	w	0.1	$\alpha_1+\alpha_2$
$5.0.\bar{1}2$	1.179	w	0.1	$\alpha_1+\alpha_2$
$6.0.\bar{1}4$	1.018	0	0.0	α_1
$7.0.\bar{1}6$	0.895	s	0.8	α_1
$8.0.\bar{1}8$	0.799	w	0.1	α_1
102	2.386	0	0.0	$\alpha_1+\alpha_2$
004	2.070	s	6.6	$\alpha_1+\alpha_2$
$10\bar{6}$	1.744	w	0.2	$\alpha_1+\alpha_2$
$20\bar{8}$	1.472	0	0.0	$\alpha_1+\alpha_2$
$3.0.\bar{1}0$	1.258	0	0.0	$\alpha_1+\alpha_2$
$4.0.\bar{1}2$	1.091	w	0.3	$\alpha_1+\alpha_2$
$5.0.\bar{1}4$	0.960	0	0.0	α_1
$6.0.\bar{1}6$	0.854	s	0.7	α_1
202	1.642	w	0.1	$\alpha_1+\alpha_2$
104	1.526	w	0.4	$\alpha_1+\alpha_2$
006	1.380	w	0.1	$\alpha_1+\alpha_2$
$10\bar{8}$	1.232	0	0.0	$\alpha_1+\alpha_2$
$2.0.\bar{1}0$	1.097	0	0.0	α_1
$3.0.\bar{1}2$	0.981	s	0.9	α_1
$4.0.\bar{1}4$	0.882	w	0.1	α_1
$5.0.\bar{1}6$	0.798	w	0.1	α_1
302	1.247	w	0.1	$\alpha_1+\alpha_2$

TABLE III—*Continued*

Indices *hkl*	Spacing calculated	Relative intensity		CuK-radiation
		observed	calculated	
204	1.193	w	0.1	$\alpha_1+\alpha_2$
106	1.118	0	0.0	$\alpha_1+\alpha_2$
008	1.035	m	0.9	α_1
1.0.$\bar{1}$0	0.951	w	0.1	α_1
2.0.$\bar{1}$2	0.872	0	0.0	α_1
3.0.$\bar{1}$4	0.800	0	0.0	α_1
402	1.003	0	0.0	α_1
304	0.998	m	0.5	α_1
206	0.932	w	0.0	α_1
108	0.882	w	0.3	α_1
0.0.10	0.828	w	0.1	α_1
502	0.838	0	0.0	α_1
404	0.821	s	1.2	α_1
306	0.795	m	0.3	α_1
20$\bar{2}$	4.190	w	0.3	$\alpha_1+\alpha_2$
30$\bar{4}$	2.980	m	10.0	$\alpha_1+\alpha_2$
40$\bar{6}$	2.204	0	0.1	$\alpha_1+\alpha_2$
50$\bar{8}$	1.723	w	0.2	$\alpha_1+\alpha_2$
6.0.$\bar{1}$0	1.407	0	0.0	$\alpha_1+\alpha_2$
7.0.$\bar{1}$2	1.186	m	1.5	$\alpha_1+\alpha_2$
8.0.$\bar{1}$4	1.023	w	0.0	α_1
9.0.$\bar{1}$6	0.900	w	0.1	α_1
10.0.$\bar{1}$8	0.802	w	0.0	α_1
30$\bar{2}$	2.405	w	0.1	$\alpha_1+\alpha_2$
40$\bar{4}$	2.095	m	3.0	$\alpha_1+\alpha_2$
50$\bar{6}$	1.767	w	0.0	$\alpha_1+\alpha_2$
60$\bar{8}$	1.490	w	0.8	$\alpha_1+\alpha_2$
7.0.$\bar{1}$0	1.272	w	0.0	$\alpha_1+\alpha_2$
8.0.$\bar{1}$2	1.102	0	0.0	$\alpha_1+\alpha_2$
9.0.$\bar{1}$4	0.968	0	0.0	α_1
10.0.$\bar{1}$6	0.862	s	1.4	α_1
40$\bar{2}$	1.652	0	0.0	$\alpha_1+\alpha_2$
50$\bar{4}$	1.542	w	0.1	$\alpha_1+\alpha_2$
60$\bar{6}$	1.397	w	0.1	$\alpha_1+\alpha_2$
70$\bar{8}$	1.248	m	1.8	$\alpha_1+\alpha_2$
8.0.$\bar{1}$0	1.112	0	0.0	$\alpha_1+\alpha_2$
9.0.$\bar{1}$2	0.993	w	0.0	α_1
10.0.$\bar{1}$4	0.892	0	0.0	α_1
11.0.$\bar{1}$6	0.807	w	0.2	α_1
50$\bar{2}$	1.252	w	0.0	$\alpha_1+\alpha_2$
60$\bar{4}$	1.203	w	0.3	$\alpha_1+\alpha_2$
70$\bar{6}$	1.130	0	0.0	$\alpha_1+\alpha_2$
80$\bar{8}$	1.048	0	0.0	α_1
9.0.$\bar{1}$0	0.963	w	0.0	α_1

TABLE III—*Continued*

Indices *hkl*	Spacing calculated	Relative intensity		CuK-radiation
		observed	calculated	
$10.0.\bar{1}2$	0.883	s	1.3	α_1
$11.0.\bar{1}4$	0.810	w	0.0	α_1
$60\bar{2}$	1.007	w	0.1	α_1
$70\bar{4}$	0.981	s	1.0	α_1
$80\bar{6}$	0.941	0	0.0	α_1
$90\bar{8}$	0.892	0	0.0	α_1
$10.0.\bar{1}0$	0.838	w	0.0	α_1
$70\bar{2}$	0.841	0	0.0	α_1
$80\bar{4}$	0.826	0	0.0	α_1
$90\bar{6}$	0.802	w	0.1	α_1

TABLE IV

Relative intensities of x-ray diffraction spots from a Weissenberg equator photograph taken with the crystal rotating around the [201] zone-axis.

Indices *hkl*	Spacing calculated	Relative intensity		CuK-radiation
		observed	calculated	
010	4.480	w	0.9	$\alpha_1+\alpha_2$
020	2.240	s	9.9	$\alpha_1+\alpha_2$
030	1.493	m	1.1	$\alpha_1+\alpha_2$
040	1.120	w	0.3	α_1
050	0.896	w	1.2	α_1
$10\bar{2}$	7.295	w	1.0	$\alpha_1+\alpha_2$
$20\bar{4}$	3.647	w	0.4	$\alpha_1+\alpha_2$
$30\bar{6}$	2.432	0	0.1	$\alpha_1+\alpha_2$
$40\bar{8}$	1.824	s	3.1	$\alpha_1+\alpha_2$
$5.0.\bar{1}0$	1.459	0	0.1	$\alpha_1+\alpha_2$
$6.0.\bar{1}2$	1.216	m	0.9	α_1
$7.0.\bar{1}4$	1.042	w	0.1	α_1
$8.0.\bar{1}6$	0.912	0	0.0	α_1
$9.0.\bar{1}8$	0.811	0	0.0	α_1
$11\bar{2}$	3.818	w	1.4	$\alpha_1+\alpha_2$
$21\bar{4}$	2.828	0	0.1	$\alpha_1+\alpha_2$
$31\bar{6}$	2.137	s	10.0	$\alpha_1+\alpha_2$
$41\bar{8}$	1.689	w	0.3	$\alpha_1+\alpha_2$
$5.1.\bar{1}0$	1.387	w	0.2	$\alpha_1+\alpha_2$
$6.1.\bar{1}2$	1.173	0	0.0	α_1
$7.1.\bar{1}4$	1.015	m	1.4	α_1
$8.1.\bar{1}6$	0.893	0	0.1	α_1
$9.1.\bar{1}8$	0.798	w	0.3	α_1
$12\bar{2}$	2.141	0	0.2	$\alpha_1+\alpha_2$

TABLE IV—*Continued*

Indices *hkl*	Spacing calculated	Relative intensity		CuK-radiation
		observed	calculated	
$22\bar{4}$	1.909	0	0.0	$\alpha_1+\alpha_2$
$32\bar{6}$	1.648	w	0.4	$\alpha_1+\alpha_2$
$42\bar{8}$	1.414	w	1.3	$\alpha_1+\alpha_2$
$5.2.\bar{1}0$	1.222	0	0.0	$\alpha_1+\alpha_2$
$6.2.\bar{1}2$	1.069	w	0.8	α_1
$7.2.\bar{1}4$	0.945	w	0.2	α_1
$8.2.\bar{1}6$	0.845	0	0.0	α_1
$13\bar{2}$	1.463	w	0.2	$\alpha_1+\alpha_2$
$23\bar{4}$	1.382	w	0.0	$\alpha_1+\alpha_2$
$33\bar{6}$	1.272	w	1.2	$\alpha_1+\alpha_2$
$43\bar{8}$	1.155	w	0.3	$\alpha_1+\alpha_2$
$5.3.\bar{1}0$	1.044	w	0.0	α_1
$6.3.\bar{1}2$	0.943	w	0.1	α_1
$7.3.\bar{1}4$	0.855	w	0.9	α_1
$8.3.\bar{1}6$	0.778	0	0.0	α_1
$14\bar{2}$	1.107	0	0.1	α_1
$24\bar{4}$	1.071	w	0.0	α_1
$34\bar{6}$	1.017	w	0.5	α_1
$44\bar{8}$	0.954	w	0.2	α_1
$5.4.\bar{1}0$	0.888	w	0.0	α_1
$6.4.\bar{1}2$	0.824	w	0.2	α_1
$15\bar{2}$	0.889	w	0.1	α_1
$25\bar{4}$	0.870	w	0.0	α_1
$35\bar{6}$	0.841	w	0.1	α_1
$45\bar{8}$	0.804	w	0.8	α_1

where 2θ denotes the angle between the incident and diffracted beams, F the structure factor, and j the number of cooperating planes. On the powder photograph the α_1 and α_2 lines were not resolved. Tables II, III, and IV contain the observed and calculated intensities of diffraction spots in three Weissenberg equator photographs taken with copper K-radiation with the crystals rotating around the *a*-, *b*-, and [201] zone-axes, respectively. The intensities I_W of the α_1 spots (where the α_1 and α_2 spots were resolved) on the Weissenberg equator films were calculated from the formula

$$I_W = \frac{1 + \cos^2 2\theta}{\sin 2\theta} |F|^2,$$

and the intensities I_W of the unresolved α_1 and α_2 spots on the same films from the formula

$$I_W = 1.5 \frac{1 + \cos^2 2\theta}{\sin 2\theta} |F|^2.$$

The atomic f-values of James and Brindley[20] were used except that in view of the replacement of part of the silver atoms by gold atoms, in place of the f-value of silver a composite value was used made up of 93 per cent of the f-value of silver and 7 per cent of the f-value of gold. No correction was made for absorption. However, small crystals were found elongated parallel to two of the rotation axes, namely, the a-axis and [201] zone-axis, with cross sections perpendicular to the rotation axes of almost equal diameters in all directions, and it is believed that in these cases any error due to the influence of crystal shape is small. The intensities used are relative and were estimated visually. For computation of a Fourier series leading to the construction of the projection of the structure on the plane 010, the intensities on the Weissenberg equator photograph taken with the crystal rotating around the b-axis were used, and these were obtained by visual comparison of the diffraction spots on the film with a standard scale of spots prepared in the Department of Chemistry of the Johns Hopkins University.[21] On this standard scale the intensities are taken to be proportional to the exposure times of the spots to a beam of constant energy output. The observed intensities obtained by comparison with the standard scale were multiplied by 2/3 for the spots in which the $\alpha_1\alpha_2$-doublet is not resolved to reduce them to the same basis as the spots due to α_1-radiation alone. The resulting values divided by the Lorentz and polarization factors yielded numbers proportional to the squares of the absolute values of the structure factors. The square roots of these numbers were extracted and positive and negative signs were affixed in accordance with those of the F's obtained from the structure arrived at by comparison of observed and calculated intensities. The experimental F-values are listed in Table V, along with the calculated F-values, which are given for comparison. The synthesis of the two-dimensional Fourier series was carried out by the method devised by Patterson[22] and improved by Patterson and Tunell.[23] The values of $A(x, y) = \rho(x, y) + K$, where $\rho(x, y)$ denotes the projected electron density and K denotes a constant, were computed at 1800 points in the half projection, corresponding to division of each of the unit cell edges into 60 parts. Vertical sections were drawn along the lines of the grid work parallel to the a-axis, and from them a contour map of $A(x, y)$ was plotted (Fig. 3). The positions of the atoms found from the contour map are as given at the beginning of this section. The largest peaks shown on the contour map are at $x=0$, $z=0$ and $x=0$, $z=\frac{1}{2}$, where the gold

[20] *Zeits. Krist.*, **78,** 475 (1931).

[21] The writer is indebted to Dr. David Harker for the use of this scale.

[22] *Phil. Mag.*, (7), **22,** 753–754 (1936).

[23] Forthcoming article in *Am. Mineral.*

TABLE V

F-values of sylvanite for *hol* planes. The upper values, obtained from an equator Weissenberg photograph,* are those used in the calculation of the Fourier projection. The lower values, given for comparison, are those calculated from the atomic positions scaled from the contour map.

l \ *h*	$\bar{11}$	$\bar{10}$	$\bar{9}$	$\bar{8}$	$\bar{7}$	$\bar{6}$	$\bar{5}$	$\bar{4}$	$\bar{3}$	$\bar{2}$	$\bar{1}$	0	1	2	3	4	5	6
18		+ 7	− 6	+11														
		+ 7.2	− 1.9	+12.4														
16	+16	+99	+13	− 9	+62	+59	− 8											
	+20.0	+68.2	+14.2	− 7.8	+56.8	+49.0	− 9.1											
14	+ 7	0	0	+10	+12	0	0	+22	0									
	+ 4.8	+ 7.6	+ 5.4	+11.4	+13.5	− 1.9	+ 4.9	+22.6	+ 3.0									
12		+105	+10	0	+42	+42	−12	+22	+71	0								
		+ 68.0	+ 7.6	− 4.6	+73.1	+50.5	−15.6	+35.6	+68.1	+ 6.2								
10		+ 7	+10	0	+ 8	0	+ 7	+15	0	0	+18	+13						
		+ 9.7	+12.2	+ 6.7	+ 9.3	+ 5.8	+ 9.3	+19.7	+ 3.7	− 3.2	+20.4	+14.5						
8			0	0	+41	+18	−10	+45	+81	0	0	+52	+22					
			+ 1.6	+ 1.7	+79.4	+47.1	−21.7	+56.7	+90.4	− 1.2	+ 6.0	+70.6	+31.7					
6			+15	0	0	+ 8	+ 6	0	0	0	+10	+ 8	0	+11	+22			
			+15.3	− 0.5	+ 5.9	+15.2	+ 9.9	+11.9	+ 7.9	+ 4.5	+20.9	+13.1	− 6.8	+11.1	+22.5			
4				0	+71	+21	−14	+29	+ 19	− 6	+ 5	+ 41	+14	−10	+44	+63		
				+ 8.2	+70.9	+31.6	−19.5	+70.5	+102.5	−13.1	+18.5	+105.0	+33.3	−13.4	+50.6	+52.7		
2					0	+20	+ 8	0	+ 7	+ 4	+ 4	+ 4	0	+ 8	+12	0	0	
					+ 5.1	+20.5	+ 5.7	+ 2.1	+15.6	+13.4	+14.4	+12.5	+ 0.9	+14.7	+20.1	− 3.2	+ 0.1	
0						+19	−12	+41	+82	−10	+ 9		+ 9	−10	+82	+41	−12	+19
						+20.7	−10.7	+62.8	+75.9	−17.6	+31.7		+31.7	−17.6	+75.9	+62.8	−10.7	+20.7

* The observed values of the intensities of $\bar{3}04$ and 004 are too low on this Weissenberg film apparently owing to an effect of the crystal shape; the observed intensities of $\bar{3}04$ and 004 on the powder photograph (cf. Table I) are in agreement with those calculated.

atoms were placed by the trial and error method; the second largest peaks are at $x=0.298$, $z=0.999$ and $x=0.277$, $z=0.235$, very close to the points

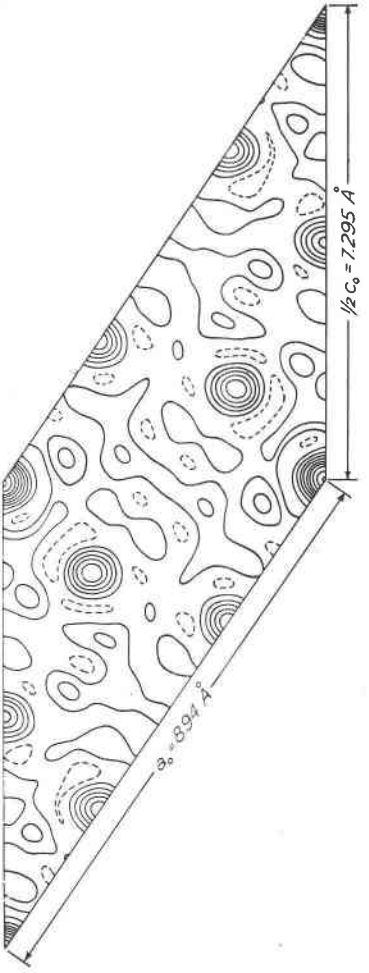

FIG. 3. Fourier projection along the symmetry axis (b-axis) of the structure of sylvanite. The contour map within the parallelogram represents the projection of one half of the unit cell. The peaks at the corners of the parallelogram represent gold atoms. The peaks midway between the corners along the vertical boundaries represent silver atoms. The peaks along the inclined boundaries and within the parallelogram represent tellurium atoms. Dotted lines are depression contours.

at which the tellurium atoms were placed by the trial and error method; the third largest peaks are at $x=0$, $z=\frac{1}{4}$ and $x=0$, $z=\frac{3}{4}$, where the silver

atoms were placed by the trial and error method. There are no other large peaks in the projection. After the contour map was drawn the intensities were recalculated from the positions of the atoms found by means of the contour map. The agreement of observed and calculated intensities is best in the case of the powder spectrum (Table I), as would be expected. The agreement of the observed and calculated intensities of the Weissenberg equator photographs (Tables II, III, and IV) is also fairly good, especially in view of the highly absorbing nature of the material. Moreover, the Fourier series calculated from the intensities of the diffraction spots on the Weissenberg equator photograph taken with the crystal rotating about the *b*-axis yielded atomic positions not differing more than 1/100 of the unit cell edge in any coordinate from those previously determined by comparison of observed and calculated intensities of the powder spectrum and the Weissenberg equator photographs taken with the crystals rotating around the *a*-axis and the [201] zone-axis. Hence the values of the parameters are believed to be correct within a tolerance of ± 0.01.

Discussion of the Atomic Arrangement

In the sylvanite structure each gold atom and each silver atom is surrounded octahedrally by six tellurium atoms and each tellurium atom is surrounded octahedrally by three tellurium atoms, two gold atoms, and one silver atom, or by three tellurium atoms, two silver atoms, and one gold atom. The orientation of the octahedra is most easily seen from Fig. 1,C. Two neighbors of each gold atom have their centers situated nearly on a line through the center of the gold atom parallel to the *a*-axis; the other four neighbors have their centers not far from a plane through the center of the gold atom perpendicular to the *a*-axis. Two neighbors of each silver atom likewise have their centers situated nearly on a line through the center of the silver atom parallel to the *a*-axis and the other four neighbors have their centers not far from a plane through the center of the silver atom perpendicular to the *a*-axis. Two neighbors of each tellurium atom also have their centers situated nearly on a line through the center of the tellurium atom parallel to the *a*-axis and the other four neighbors have their centers not far from a plane through the center of the tellurium atom perpendicular to the *a*-axis. The distances between the gold and tellurium atoms are 2.67 Å, 2.76 Å, and 3.26 Å. The distances between the silver and tellurium atoms are 2.69 Å, 2.94 Å, and 3.19 Å. The distances between tellurium atoms are 2.88 Å, 3.56 Å, 3.64 Å,[24] and 3.64 Å. All these distances are shown in Fig. 1,C. The struc-

[24] The two distances 3.64 Å are not required by symmetry to be the same.

ture can be described as consisting of lines of atoms parallel to the a-axis. These lines are at $y=0$, $z=0$, at $y=0.433$, $z=\frac{1}{4}$, at $y=0$, $z=\frac{1}{2}$, and at $y=0.567$, $z=\frac{3}{4}$. Along these lines metal atoms are separated by pairs of tellurium atoms, the metal atoms lying exactly on the lines and the tellurium atoms lying close to them. The metal atoms also lie in planes parallel to the b- and c-axes at $x=0$ with two layers of tellurium atoms separating the metal atoms.